Journal of Integrative Agriculture 2026, 25(1): 339–351

Available online at ScienceDirect

Journal of Integrative Agriculture

RESEARCH ARTICLE

Matrix effect of hydroxycinnamic acids on chromatic properties and phenolic profile of Cabernet Sauvignon dry red wine

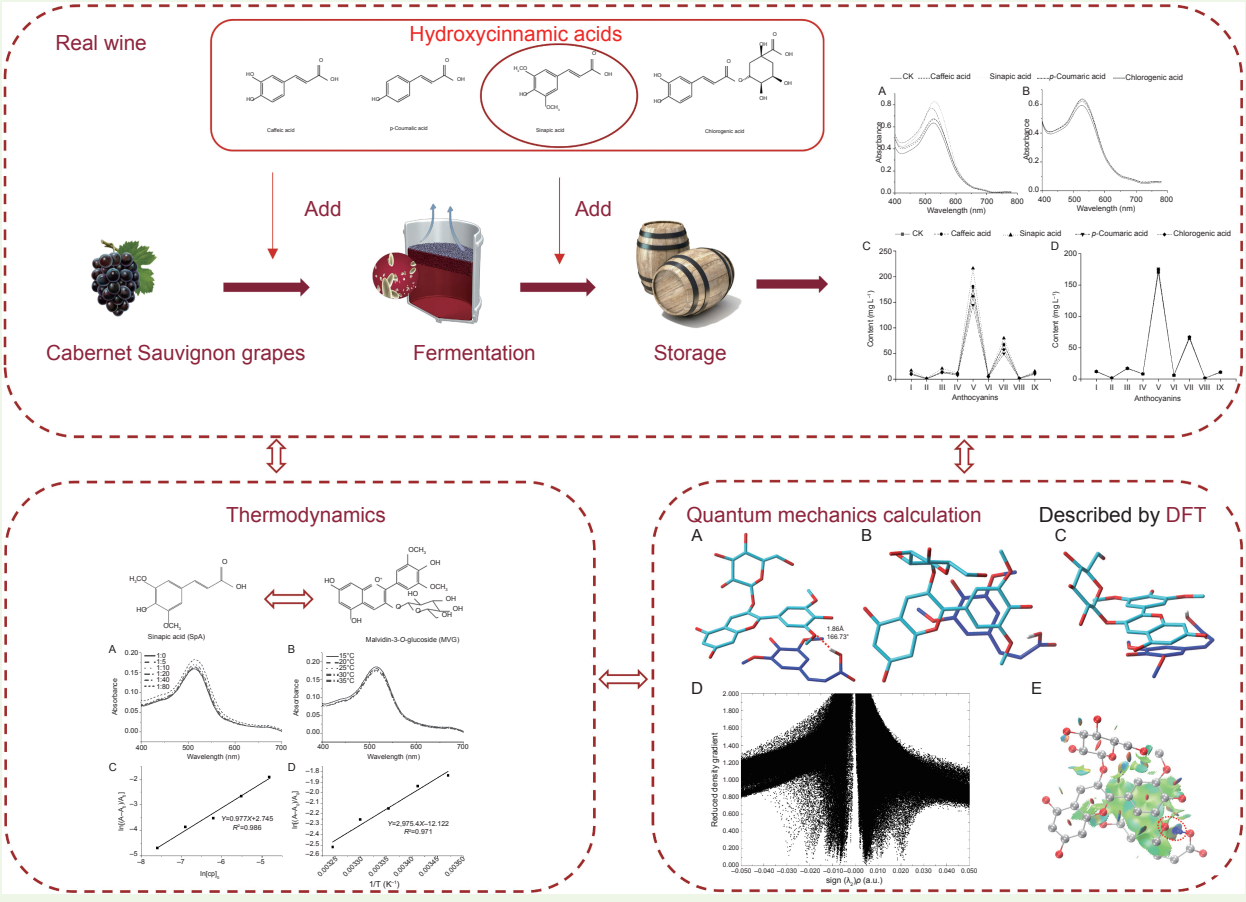
Lulu Wu[1], Yu Zhang[1], Mario Prejanò[2], Tiziana Marino[2], Nino Russo[2], Guojie Jin[1, 3], Yongsheng Tao[1, 3], Yunkui Li[1, 3#]

[1] *College of Enology, Northwest A&F University, Yangling 712100, China*
[2] *Dipartimento di Chimica e Tecnologie Chimiche, Università della Calabria, Arcavacata di Rende 87036, Italy*
[3] *Ningxia Helan Mountain's East Foothill Wine Experiment and Demonstration Station, Northwest A&F University, Yongning 750104, China*

Highlights

- Hydroxycinnamic acids can enhance the color quality of wine through copigmentation.
- Copigmentation is driven by hydrogen bonding and dispersion forces.
- The anthocyanin backbone and the carboxyl group of sinapic acid are the key sites.

Graphical abstract



Received 10 January 2025; Received in revised form 1 August 2025; Accepted 23 September 2025; Available online 27 October 2025
#Correspondence Yunkui Li, Tel: +86-29-87092107, Fax: +86-29-87092991, E-mail: ykli@nwsuaf.edu.cn

© 2026 CAAS. Publishing services by Elsevier B.V. on behalf of KeAi Communications Co. Ltd. This is an open access article under the CC BY-NC-ND license (http://creativecommons.org/licenses/by-nc-nd/4.0/). Peer review under responsibility of Editorial Board of *Journal of Integrative Agriculture*.
doi: 10.1016/j.jia.2025.10.013

Abstract

The effect of adding hydroxycinnamic acids (caffeic acid, sinapic acid, *p*-coumaric acid and chlorogenic acid) in Cabernet Sauvignon dry red wine before and after fermentation was investigated, taking into account the color parameters, anthocyanin content, and overall polyphenol levels in the wine samples. The copigmentation effect of malvidin-3-*O*-glucoside and sinapic acid was further explored in model solution and through theoretical calculations. The results indicated that the addition of hydroxycinnamic acids significantly enhanced the wine's color with sinapic acid (before the fermentation) showing the most pronounced color protection effect. Compared to control samples, the addition of hydroxycinnamic acids resulted in a 36% increase in total phenolic content and a 28% increase in total anthocyanin content. Thermodynamic analysis revealed that the interaction between sinapic acid and malvidin-3-*O*-glucoside was spontaneous and exothermic. Theoretical studies identified hydrogen bonding (HB) and dispersion forces as the main primary stabilizing forces, with the carboxyl group of sinapic acid playing a critical role while the anthocyanin backbone also influenced the interaction.

Keywords: matrix effect, dry red wine, polyphenol, hydroxycinnamic acids, anthocyanins

1. Introduction

Color is a key metric for evaluating the quality of red wine, offering insights into grape variety, winemaking practices, and the wine's stage of aging and maturity (Fanzone *et al.* 2015) and shaping consumer perception (Bimpilas *et al.* 2016).

Anthocyanins, the most important pigments in vascular plants, are natural colorants with promising applications and unique physiological functions (Sun *et al.* 2019). Several studies have shown that anthocyanins possess antioxidant, anti-inflammatory, antidiabetic, and anti-aging effects (Kent *et al.* 2017). As major polyphenolic constituents of grapes and wines, anthocyanins significantly influence the chromatic characteristics of red wines (Peri *et al.* 2015; Fan *et al.* 2023a).

During winemaking and aging, changes in the quantity and type of anthocyanins can occur, including the degradation of monomeric anthocyanins and the formation of acylated and polymerized anthocyanins through copigmentation, cycloaddition, polymerization and oxidation (Alcalde-Eon *et al.* 2006). These transformations are influenced by the molecular structure of anthocyanins and the substrates of wine samples (Liu *et al.* 2015). Copigmentation refers to the formation of stable complexes by anthocyanins through intermolecular stacking, hydrogen bonding (HB), and complexation with other colorless organic molecules or metal ions (Escribano-Bailon and Santos-Buelga 2012), which changes the molecular properties, thereby achieving increased stability. It has been found that copigmentation contributes 30−50% of the color in young red wines, while in aged one the contribution range from 8−30% (Boulton 2001). A wide range of wine constituents can act as copigments that enhance the stability of the floral chromosome, including organic acids, metal ions, phenolic compounds (flavonoids, phenolic acids, alkaloids), polysaccharides (e.g., gum arabic, guar gum, pectin, chitosan, alginate), and proteins (e.g., amino acids, casein, whey proteins, soy proteins, and mannoproteins) (González-Manzano *et al.* 2009; Liu *et al.* 2025a).

Polyphenolic compounds constitute a fundamental component of the wine matrix and play a pivotal role throughout the fermentation and aging processes, exerting a critical impact on wine color quality (Liu *et al.* 2025b; Wu *et al.* 2025). They are currently attracting great interest due to the structures have a broad π-conjugated system which facilitates binding to the anthocyanins *via* π–π stacking (Trouillas *et al.* 2016; Liu *et al.* 2025c). Such interactions typically adopt a "sandwich-like" structure, which shields the flavylium cation from nucleophilic attack by water, thereby enhancing pigment stability and preventing chromatic decay (Teixeira *et al.* 2013; Wu *et al.* 2026). According to their structural characteristics, wine phenolics are classified into non-flavonoids and flavonoids. Flavonoids possess a characteristic C6-C3-C6 carbon skeleton (Ignat *et al.* 2011) and can be divided into flavonols, flavanols, and anthocyanins (Fontana *et al.* 2013). Non-flavonoid substances primarily include phenolic acids and stilbenes, with phenolic acids being more abundant in wine. Phenolic acids are categorized into hydroxybenzoic acids, which have a C6-C1 skeleton, and hydroxycinnamic acids, characterized by a C6-C3 skeleton (Lingua *et al.* 2016).

A variety of hydroxycinnamic acids, including chlorogenic acid, sinapic acid, ferulic acid, *p*-coumaric acid, and caffeic acid, are generally recognized as effective copigments, exhibiting potency similar to that of flavanols and dihydroflavonols (Fanzone *et al.* 2015). Both experimental and computational studies have revealed that hydroxycinnamic acids generally exhibit stronger copigmentation effects than hydroxybenzoic acids (Zhang *et al.* 2015b). It was speculated that the reason may be that acrylic acid has a longer carbon chain than formic acid, which is more conducive to the combination of copigment and anthocyanin (Zhang *et al.* 2015b).

This study aims to explore the copigmentation of hydroxycinnamic acids under real wine fermentation conditions. Among the tested compounds, sinapic acid, commonly found in real wines, was copigment of malvidin-3-*O*-glucoside investigating the thermodynamic nature of the effect in a model wine. Quantum mechanics (QM) calculation was applied to explore the intermolecular mechanisms of copigmentaion effect, focusing on their structural and energetic properties. It is expected to further explore and explain the color protection ability of polyphenols, provide theoretical and technical support for the improvement of dry red wine color protection.

2. Materials and methods

2.1. Raw materials for winemaking

The raw materials used in the winemaking are Cabernet Sauvignon grapes from Ningxia Hui Autonomous Region, China. The reduced sugar g L^{-1} and total acid content of raw materials were 270 g glucose L^{-1} and 6.2 g tartaric acid L^{-1}.

2.2. Chemicals

Hydroxycinnamic acids, including sinapic acid, caffeic acid, *p*-coumaric acid, and chlorogenic acid, were purchased from Shanghai Aladdin Biochemical Technology Co., Ltd. The anthocyanin standard, malvidin-3-*O*-glucoside, was supplied by SHANGHAI ZZBIO Co., Ltd. The *Saccharomyces cerevisiae* (Angel Yeast Co., Ltd., China) and pectinase (Lallemand, CA, USA) were prepared for winemaking. All other chemicals used in the experiments were purchased from Tianjin Kemiou Chemical Reagent Co., Ltd., China.

2.3. Winemaking

Harvested from Ningxia, China, fully ripe grapes were sorted, destemmed, and crushed before being placed in ten tanks. Then, *Saccharomyces cerevisiae* (200 mg L^{-1}), pectinase (20 mg L^{-1}) and sulfur dioxide (60 mg L^{-1}) were added to initiate fermentation. All wine samples were divided into ten groups, including five groups receiving pre-fermentation treatment with hydroxycinnamic acids and five groups receiving post-fermentation treatment with the same compounds. One group without any hydroxycinnamic acid served as the control (CK), while the remaining samples were supplemented with 360.32 mg L^{-1} caffeic acid, 448.42 mg L^{-1} sinapic acid, 328.32 mg L^{-1} *p*-coumaric acid, and 708.62 mg L^{-1} chlorogenic acid, respectively. At the end of fermentation, all samples were filtered and bottled for further analysis.

2.4. Determination of general parameters of wine

General parameters of the wine samples were determined following the protocols outlined in the *Compendium of International Methods of Analysis of Musts and Wines*, including pH value of samples, alcohol content (% vol), reduced sugar (g glucose L^{-1}), total acid (g tartaric acid L^{-1}), volatile acid (g acetic acid L^{-1}) and free sulfur dioxide (mg L^{-1}).

2.5. Optical and chromatic feature

The optical characteristics of the wine samples were evaluated using a UV–Visible spectrophotometer (UV-1780, SHIMADZU, Japan). Absorbance spectra were recorded over the wavelength range of 400–780 nm at 1 nm intervals using a 1 mm pathlength quartz cuvette, with distilled water as the reference.

Based on the absorption spectrum, absorbance values (A_{630}, A_{570}, A_{520}, and A_{450}) were selected to obtain the chromatic parameters, including L^* (lightness), a^* (green/red), b^* (blue/yellow), h_{ab} (hue dependency), C^*_{ab} (saturation dependency), and ΔE^*_{ab} (total color difference) of wine samples (Gonnet 1999).

The feature color of wine samples can visualize the macroscopic color characterization compared with the parameters calculated from the absorbance of the visible absorption spectrum (Fan *et al.* 2023b).

2.6. Polyphenol content analysis

The content of total phenolics, flavonols, anthocyanins were measured, following previous suggestions (Cliff *et al.* 2007), using wine (0.5 mL) sample diluted with 10% ethanol (4.5 mL). The diluted samples (0.25 mL) were added with 2% HCl (4.55 mL) and 95% ethanol-0.1% HCl (0.25 mL). After shaking and mixing, the samples were allowed to stand for 15 min to ensure homogeneity and stability. The absorbance of wine samples was measured at 280, 360 and 520 nm with 1 mm cuvette. Absorbance readings (A_{280}, A_{360} and A_{520}) corresponded to total phenolic, flavonols, and anthocyanin content. The *p*-DMACA method was applied to determine flavanols (Arnous *et al.* 2002).

2.7. Anthocyanin form analysis

The proportions of anthocyanins into monomeric, copigmented, and polymeric forms was analyzed using the method adapted from Mazza *et al.* (1999). To assess A_{acet}, the wine sample (2 mL) was prepared with a 10% (v/v) acetaldehyde solution (20 μL) and then incubated at room temperature for 45 min. For A_{SO_2}, the wine sample (2 mL) was mixed with a 5% (w/v) SO_2 solution (60 μL), and measurements were taken after 10 min. Additionally, the wine sample was diluted tenfold with model wine to measure A_{520}. The A_{acet}, A_{SO_2}, and A_{520} were the absorbance values of the prepared samples at 520 nm using a 1 mm pathlength quartz cuvette. The proportion of anthocyanins in different forms was calculated using eqs. (1)–(3):

$$\text{Copigmented anthocyanin (\%)}=\left[\frac{(A_{acet}-A_{520})}{A_{acet}}\right]\times 100 \quad (1)$$

$$\text{Monomeric anthocyanin (\%)}=\left[\frac{(A_{520}-A_{SO_2})}{A_{acet}}\right]\times 100 \quad (2)$$

$$\text{Polymeric anthocyanin (\%)}=\left[\frac{A_{SO_2}}{A_{acet}}\right]\times 100 \quad (3)$$

2.8. Monomeric anthocyanin analysis

The monomeric anthocyanins were quantified using high-performance liquid chromatography (HPLC, LC-20A, SHIMADZU, Japan), with wine samples pre-filtered through a water filtration membrane (0.22 μm) as pretreatment. Mobile phase A consisted of formic acid, acetonitrile, and purified water in a volume ratio of 1:4:32, while mobile phase B had the same composition with a different ratio (1:20:16). The LC Column (4 μm, 250 mm×4.6 mm) was used as the chromatographic column. The gradient elution program was as follows: 0–45 min, 0–35% B; 45–46 min, 35–100% B; 46–50 min, 100% B; 50–51 min, 100–0% B; and 51–55 min, 0% B. The column temperature was maintained at 35°C, and detection was performed at a wavelength of 520 nm. The sample injection volume was set to 20 μL, with a flow rate of 1.0 mL min^{-1}.

Anthocyanins were identified based on their retention times and maximum absorption wavelengths, with each

chromatographic peak corresponding to a specific anthocyanin. The quantification of anthocyanins was obtained using the formula y=0.000002x+0.1768. The peak area of different anthocyanins is "x", and the content of anthocyanins (mg L^{-1}) is "y". The malvidin-3-*O*-glucoside was used as the standard in the measurement.

2.9. Preparation of model wine solutions

To ensure an ionic environment similar to that of real wines, 5 g L^{-1} of tartaric acid and 12% (v/v) ethanol were added to the model wine, and the pH was adjusted to 3.6. Sodium chloride was added to adjust the ionic strength to 0.2 mol L^{-1}. Malvidin-3-*O*-glucoside was dissolved in a 0.1 mmol L^{-1} model wine solution to prevent self-association, followed by dilution with specific volumes of copigment solution to achieve molar ratios of 1:0, 1:5, 1:10, 1:20, 1:40, and 1:80 for sinapic acid/malvidin-3-*O*-glucoside at 20°C. To assess the effect of temperature on copigmentation behavior, additional model solutions with a fixed molar ratio of 1:40 were incubated at 15, 20, 25, 30, and 35°C. All samples were equilibrated in the dark for 30 min and prepared in triplicate.

2.10. Measurement of copigmentation magnitude and thermodynamic parameters

According to the methodology described by Boulton (2001), the extent of copigmentation was quantified by measuring the hyperchromic effect and bathochromic shift. Absorption spectra of the model wine samples were recorded from 400 to 780 nm at 1 nm intervals using a 1 cm pathlength quartz cuvette, with distilled water as the reference. The hyperchromic effect and bathochromic shift were calculated as $(A–A_0)/A_0$ and $\Delta\lambda_{max}=\lambda_{max}–\lambda_0$, respectively, where A_0 is the absorbance of malvidin-3-*O*-glucoside at λ_0, A is the absorbance of the copigmentation solution (sinapic acid/malvidin-3-*O*-glucoside) at λ_0, and λ_{max} represents the maximum absorption of the copigmentation solution (sinapic acid/malvidin-3-*O*-glucoside).

The thermodynamic parameters of the copigmentation process were calculated according to the reported method (Brouillard *et al.* 1989). The enthalpy (ΔH), entropy changes (ΔS), Gibbs free energy (ΔG), and equilibrium constant (K) for the copigmentation reaction were determined using eqs. (4)–(7) as described by Lambert *et al.* (2011).

$$\ln\left(\frac{A–A_0}{A_0}\right)=\ln K+n\ln[cp]_0 \quad (4)$$

$$\Delta G=–RT\times\ln K \quad (5)$$

$$\Delta G=\Delta H–T\Delta S \quad (6)$$

$$\ln\left(\frac{A–A_0}{A_0}\right)=–\frac{\Delta H}{RT}+\frac{\Delta S}{R}+n\ln[cp]_0 \quad (7)$$

where n is the stoichiometric ratio of anthocyanin to sinapic acid $[cp]_0$ is the concentration of sinapic acid added to the anthocyanin solution, R is the gas constant (8.314 J mol^{-1} K^{-1}), and K is absolute temperature in Kelvin.

2.11. Quantum mechanics calculation

To investigate the molecular conformations and interaction mechanisms between malvidin-3-*O*-glucoside and sinapic acid, we adopted the approach described by Li *et al.* (2018). This method was used to explore the conformational space and identify the optimal copigmentation conformer(s). The geometries of these conformers were optimized using the dispersion-corrected hybrid functional B3LYP-D3 (Grimme *et al.* 2010) with the 6-31+G(d) basis set, which includes polarization and diffusion functions for heavy atoms. To ensure that each structure corresponded to a true energy minimum, vibrational frequency calculations were performed. These calculations also provided corrections for thermodynamic parameters. Additionally, the solvent effects on molecular structures were incorporated using the Integral Equation Formalism Polarizable Continuum Model (IEFPCM) (Li *et al.* 2018, 2019), simulating the interaction between malvidin-3-*O*-glucoside and sinapic acid in aqueous solution.

To further refine the thermodynamic properties of copigmentation, the B3PW91-D3 hybrid functional, combined with the IEFPCM implicit solvation model and the aug-cc-pVDZ basis set, was employed. Additionally, the counterpoise correction method was applied to account for Basis Set Superposition Error (BSSE) at the same computational level (Simon *et al.* 1996).

The binding energies, including Gibbs free energy (ΔG), thermal energy (ΔE), and enthalpy (ΔH) for each conformer, were calculated using the following equation:

$$\Delta E_{binding}=E_{complex}–E_{pigment}–E_{copigment} \quad (8)$$

To compare the conformers within the copigmentation complex, Boltzmann weights (BW) were determined based on their relative Gibbs free energies.

Intermolecular non-covalent interactions were visualized using Multiwfn 3.8 (Lu and Chen 2012) and VMD 1.9 (Humphrey *et al.* 1996). All computations were executed using the Gaussian 09 software package (Frisch *et al.* 2009).

2.12. Statistical analysis

All data were expressed as mean±standard deviation. One-way analysis of variance (ANOVA) with SPSS software (version 19.0; SPSS Inc., Chicago, IL, USA), and mean comparisons were conducted through Duncan's multiple range test. Graphical representations were generated using Origin 2024 software (OriginLab, Northampton, MA, USA).

3. Results

3.1. General enological parameters

Appendix A shows the pH, total acid, volatile acid, reduced sugar, ethanol content, free SO_2 of the samples after the treatment with four hydroxycinnamic acids at two different stages.

As indicated in Appendix A-a, all the indices complied with the Wine National Standard GB/T 15037-2006. When hydroxycinnamic acids were added before fermentation, the differences in pH, volatile acid and alcohol content of the treated samples were smaller compared to CK. In addition, the total acid in the hydroxycinnamic acid treated wine samples decreased, the reduced sugar content increased, and free SO_2 in the chlorogenic acid treated wine samples decreased by 5.13 mg L^{-1} compared to CK.

As shown in Appendix A-b, the values of all indicators were

within the normal range. The changes in pH, volatile acid, reduced sugar and alcohol content of the wine samples after fermentation with four hydroxycinnamic acids were minimal, indicating that the correlation between the indicators and the treatments was not significant. Compared with CK, the total acid and free SO_2 of the treated-samples showed slight increases.

3.2. Chromatic feature

The absorption spectra (400–780 nm) of wine samples treated with different phenolic acids are shown in Fig. 1, covering both pre- and post-fermentation additions. In particular, Fig. 1-A illustrates four hydroxycinnamic acid treatments prior to fermentation. Compared with CK, the maximum absorbance of each treated group increased, and a bathochromic shift occurred, especially in the sample containing sinapic acid. As shown in Fig. 1-B, the maximum absorbance of treated samples also increased, but the differences between the groups were not significant.

Table 1 presents the color parameters (L^*, a^*, b^*, C^*_{ab} and h_{ab}) of wine samples before fermentation. The L^* values of all the wine samples ranged from 62.40 to 69.28, with all treated samples showing a decrease in lightness compared with CK, suggesting darker wine color. Sinapic acid caused the most pronounced darkening, followed by

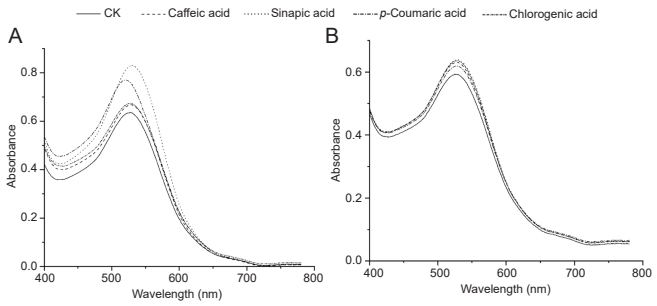


Fig. 1 Visible spectra of real wine samples treated with hydroxycinnamic acids before fermentation (A) and after fermentation (B).

p-coumaric acid, chlorogenic acid, and caffeic acid. The a^* value of each sample is between 35.29 and 43.35, indicating a significant difference among wine samples. Among them, the a^* value of sinapic acid treatment is the largest, indicating that its redness was the heaviest, which was also consistent with its deepest color. The range of b^* value is between –3.42 and 4.61, and the smallest b^* value was obtained for the wine sample with added sinapic acid. C^*_{ab} value represents the color saturation of the wine, and increases in all treatment groups compared to CK, indicating that different hydroxycinnamic acids additions to the samples before the fermentation resulted in more saturated color, with the best effect being sinapic acid, followed by *p*-coumaric acid. Generally speaking, the h_{ab} value of red wines ranges from 0° to 90°, and h_{ab} of each sample ranges from –4.51° to 6.65°. As far as CIELAB parameters are concerned, all four different hydroxycinnamic acids additions to the wine samples before the fermentation positively affected the color of the wine samples compared to CK, and sinapic acid had the best effect.

The color parameters after fermentation are presented in Table 1. For the L^* values, the addition of four different hydroxycinnamic acids to the wine samples after fermentation resulted in varying degrees of decrease compared to CK, with the largest decrease of 2.1 a.u. occurring with sinapic acid. The change in the a^* values indicated that the redness of all treatment samples was more pronounced, particularly in the sample containing sinapic acid, followed by chlorogenic, caffeic, and *p*-coumaric acids. The b^* values exhibited the same trend as L^*. The C^*_{ab} valuesranged from 29.24 to 31.01, following the order: sinapic acid>chlorogenic acid>caffeic acid>*p*-coumaric acid>CK. As illustrated in Table 1, it can be obtained that the wine samples with hydroxycinnamic acids can make their h_{ab} decreased and had better trend. In general, the samples treated with caffeic acid, sinapic acid, *p*-coumaric acid and chlorogenic acid after the fermentation resulted in better development, but the effect was not very significant compared to adding them before the fermentation.

Table 1 CIELAB parameters (L^*, a^*, b^*, C^*_{ab}, h_{ab}) and characteristic color of real wine samples treated with hydroxycinnamic acids at different fermentation stages

	CK	Caffeic acid	Sinapic acid	*p*-Coumaric acid	Chlorogenic acid
Before fermentation					
L^*	69.28±0.49 a	67.49±0.05 b	62.40±0.30 d	65.40±0.13 c	67.01±0.49 b
a^*	35.29±0.73 c	36.16±0.00 c	43.35±0.24 a	39.58±0.03 b	35.53±0.22 bc
b^*	–0.22±0.36 d	0.91±0.06 c	–3.42±0.05 e	4.61±0.01 a	1.59±0.03 b
C^*_{ab}	35.29±0.73 c	36.17±0.00 c	43.48±0.24 a	39.85±0.03 b	35.56±0.22 c
h_{ab}/°	–0.35±0.07 e	1.44±0.09 c	–4.51±0.09 e	6.65±0.02 a	2.57±0.06 b
Characteristic color					
After fermentation					
L^*	68.68±0.01 a	67.05±0.04 c	66.58±0.06 e	67.33±0.06 b	66.83±0.04 d
a^*	29.22±0.02 d	30.64±0.08 b	31.01±0.07 a	29.84±0.02 c	30.96±0.04 a
b^*	1.10±0.03 a	0.25±0.00 b	–0.37±0.05 d	0.34±0.09 b	0.01±0.02 c
C^*_{ab}	29.24±0.02 d	30.64±0.08 b	31.01±0.06 a	29.84±0.02 c	30.96±0.04 a
h_{ab}/°	2.16±0.06 a	0.48±0.01 b	–0.68±0.10 d	0.66±0.17 b	0.01±0.03 c
Characteristic color					

Different letters on the same line indicate significant differences, $P<0.05$.

3.3. Phenolic content and anthocyanin form analysis

Table 2 presents the concentrations of various phenolic compounds following the addition of hydroxycinnamic acids to the wine samples at different periods.

The total phenolic content of the wine samples treated with four hydroxycinnamic acids increased significantly. The increase ranged from 25 to 46%, and the highest total phenolic content (2,690.71 mg L^{-1}) occurred in the *p*-coumaric acid-treated sample. In addition, although only the phenolic acids were added before fermentation, the content of flavonols also significantly increased in each treatment compared with CK. The content of flavanols in the samples treated with *p*-coumaric acid, caffeic acid, chlorogenic acid, and sinapic acid increased by 40, 61.43, 61.43, and 122.66 mg L^{-1}, respectively. Furthermore, there was a significant difference in the content of flavanols among the treated samples. Except for a slight decrease in the chlorogenic acid-treated samples, the other treatment groups showed a significant increase, with the highest content of 546.49 mg L^{-1} observed in the *p*-coumaric acid-treated sample. The content of anthocyanins in the sample with sinapic acid reached 334.08 mg L^{-1}, reflecting an increase of 28% compared with CK. Regarding the percentage of anthocyanins, the results of the wine samples varied among the treatment groups. Among them, the proportions of copigmented anthocyanins in caffeic acid and sinapic acid treated samples increased, but the changes were not significant. The monomeric anthocyanins in the chlorogenic acid-treated sample were on the rise, while a significant increase in polymeric anthocyanins was observed in the *p*-coumaric acid-treated sample.

In Table 2, the differences observed in the samples treated with phenolic acids after fermentation are presented. Firstly, the total phenolic content of each treatment group was significantly increased compared to the control group, in the order of: *p*-coumaric acid>caffeic acid=chlorogenic acid>sinapic acid. Also, the flavonols content of the four hydroxycinnamic acids treatment groups were higher than that of CK, with increases ranging from 8.57 to 94.29 mg L^{-1}. Unlike the situation before the fermentation, the flavanols content was decreasing in all treatment groups. Secondly, the changes in the proportions of anthocyanins can be seen that the copigmented anthocyanins of *p*-coumaric acid and chlorogenic acid treatment samples were increasing. In contrast, the monomeric anthocyanins of caffeic and erucic acid treated samples were decrease, the changes were not significant, and further storage is needed to assess the effects of the treatment groups.

3.4. Monomeric anthocyanins

The types and concentrations of anthocyanins in wine samples were determined using HPLC, and five monosaccharide anthocyanins and four acylated anthocyanins were detected, as shown in Fig. 2.

As illustrated in Fig. 2-A, the addition of phenolic acids before fermentation resulted in significant differences in anthocyanin content across treatment groups. Among the nine monomeric anthocyanins, malvidin-3-*O*-glucoside and malvidin-3-*O*-acetyl-glucoside were the most abundant due to their more stable structure. Compared with CK and other treatments, the content of all types of anthocyanins in the sinapic acid-treated samples was significantly higher, which is also consistent with their superior chromatic characteristics. The amounts of delphinidin-3-*O*-glucoside, cyanidin-3-*O*-glucoside, petunidin-3-*O*-glucoside, malvidin-3-*O*-glucoside, and malvidin-3-*O*-coumaroyl-glucoside with outstanding growth increased by 45.29, 65.31, 42.14, 21.44, and 37.58%, respectively, compared to CK.

Fig. 2-B reports the data obtained after fermentation and, in contrast to the data obtained before fermentation, shows no significant differences. The content of malvidin-3-*O*-glucoside in caffeic acid, chlorogenic acid, and *p*-coumaric acid-treated samples increased by 1.87, 4.05, and 5.67 mg L^{-1}, respectively, compared to CK.

3.5. Copigmentation thermodynamic data

Based on the observation that the addition of hydroxycinnamic

Table 2 Phenolic composition and anthocyanin distribution in wine samples treated with hydroxycinnamic acids at different fermentation stages

Content	CK	Caffeic acid	Sinapic acid	*p*-Coumaric acid	Chlorogenic acid
Before fermentation					
Total phenolics (mg gallic acid L^{-1})	1,837.14±10.10 d	2,522.86±10.10 b	2,505.00±5.05 b	2,690.71±5.05 a	2,305±5.05 c
Flavonols (mg quercetin L^{-1})	131.71±2.02 d	193.14±4.04 b	254.57±2.02 a	171.71±2.02 c	193.14±0.00 b
Flavanols (mg catechin L^{-1})	464.02±0.44 d	484.54±1.17 c	506.39±2.33 b	546.49±7.73 a	450.72±0.00 d
Anthocyanins (mg malvidin-3-glucoside L^{-1})	260.61±1.44 c	266.73±1.44 b	334.08±1.44 a	250.41±1.44 d	237.14±0.00 e
Copigmented anthocyanin (%)	32.02±0.74 a	34.67±0.15 a	36.54±0.41 a	23.83±0.70 b	26.20±0.43 b
Monomeric anthocyanin (%)	37.49±0.68 ab	34.48±0.23 bc	36.40±0.36 ab	29.56±0.48 c	40.17±0.42 a
Polymeric anthocyanin (%)	30.49±0.07 c	30.85±0.09 c	27.06±0.05 d	46.62±0.22 a	33.63±0.01 b
After fermentation					
Total phenolics (mg gallic acid L^{-1})	1,958.57±10.1 d	2,576.43±5.05 b	2,187.14±0 c	2,780.00±0.00 a	2,576.43±5.05 b
Flavonols (mg quercetin L^{-1})	124.57±4.04 d	184.57±0.00 b	186.00±2.02 b	133.14±0.00 c	218.86±0.00 a
Flavanols (mg catechin L^{-1})	700.82±0.58 a	674.02±0.00 b	666.08±0.44 c	666.08±1.31 c	642.68±0.58 d
Anthocyanins (mg malvidin-3-glucoside L^{-1})	255.51±2.89 b	261.63±0.00 a	257.55±0.00 ab	261.63±0.00 a	255.51±0.00 b
Copigmented anthocyanin (%)	36.46±0.83 b	32.90±0.96 c	35.16±0.90 bc	37.99±0.87 ab	40.66±0.45 a
Monomeric anthocyanin (%)	32.66±0.91 ab	36.29±0.96 a	33.79±0.94 ab	32.49±1.03 b	30.82±0.32 b
Polymeric anthocyanin (%)	30.88±0.07 a	30.81±0.01 a	31.05±0.04 a	29.53±0.16 b	28.52±0.13 c

Different letters on the same line indicate significant differences, $P<0.05$.

acid to real wines can significantly enhance their color profile, the prominent hydroxycinnamic acid, sinapic acid, and the representative anthocyanin, malvidin-3-*O*-glucoside, were selected to investigate the copigmentation process in model wines.

As illustrated in Fig. 3, the visible absorption spectra of sinapic acid/malvidin-3-*O*-glucoside solution with varying molar ratios under different temperatures was measured to analyzed the impact of sinapic acid on the spectral characteristics of anthocyanin. The absorption intensities observed for the experimental group (molar ratios of 1:5, 1:10, 1:20, 1:40, and 1:80) exceeded those of the control group (molar ratio of 1:0). Upon incremental addition of sinapic acid to the model wine solution, a significant enhancement in absorption was observed across the visible spectrum, particularly near 520 nm. The absorption increased proportionally with the quantity of sinapic acid introduced. In contrast, temperature exhibited a comparatively minor effect on the absorption profile.

The spectral modifications induced by sinapic acid were further quantified in terms of hyperchromic effect and bathochromic shift, derived from the spectral data in Fig. 3. The hyperchromic effect intensified, and the bathochromic shift increased with rising molar ratios, reaching a maximum at a ratio of 1:80, as shown in Appendix B. However, at lower sinapic acid concentrations (molar ratios below 1:20), the copigmentation effect remained statistically insignificant (P>0.05).

Thermodynamic parameters provide insights into the possibility of interactions and enable the prediction of energy exchanges between anthocyanins and copigments. Using UV-Vis spectroscopy, the intercept (ln$K$) and slope (n) were obtained from the linear regression of $\ln[(A-A_0)/A_0]$ against $\ln[cp]_0$. The resulting plot displayed strong linearity (R^2=0.986), yielding K=15.56 mol L^{-1}, consistent with prior findings (Wu *et al.* 2024a). The K quantifies the strength of the copigmentation interaction between malvidin-3-*O*-glucoside and sinapic acid. The stoichiometric constant (n=0.977) closely approximates 1, indicating a 1:1 binding stoichiometry between malvidin-3-*O*-glucoside and sinapic acid.

The Gibbs free energy variation (ΔG=–1.63 kcal mol^{-1}) was negative, indicating that the copigmentation process proceeds spontaneously. The enthalpy change (ΔH=–5.91 kcal mol^{-1}) was derived from the slope of the linear plot of $\ln[(A-A_0)/A_0]$ versus the reciprocal temperature ($1/T$), while entropy change (ΔS=–60.14 J K^{-1} mol^{-1}) was obtained by the equation, $\Delta G=\Delta H-T\Delta S$. The negative ΔG and ΔH values suggest that HB and van der Waals forces are key contributors to the spontaneous interaction (Zhang *et al.* 2015a). Meanwhile, the negative ΔS may reflect the influence of hydrophobic effects and π–π stacking interactions in the binding process.

3.6. QM investigation of the intermolecular copigmentation between sinapic acid and malvidin-3-*O*-glucoside

In order to better understand the intermolecular mechanism betweent sinapic acid and malvidin-3-*O*-glucoside (Appendix C), we performed QM calculations of density functional theory (DFT) to gain insights on their interaction. By scanning the interaction potential energy surface, the optimal conformation of sinapic acid/malvidin-3-*O*-glucoside was found. The mechanism was dissected from the structural features of the system, visual demonstration and energy analysis.

Performance of the structural characteristics of the copigmentation system Seven low-energy conformers were identified through a comprehensive scan of the conformational space. The geometry of the copigmentation complexes are illustrated in Fig. 4 (conformer 6, the most predictable structure) and Appendix D (the other six conformers) labeled with detailed stacking parameters. Two stacking modes of the copigmentation complex were found:

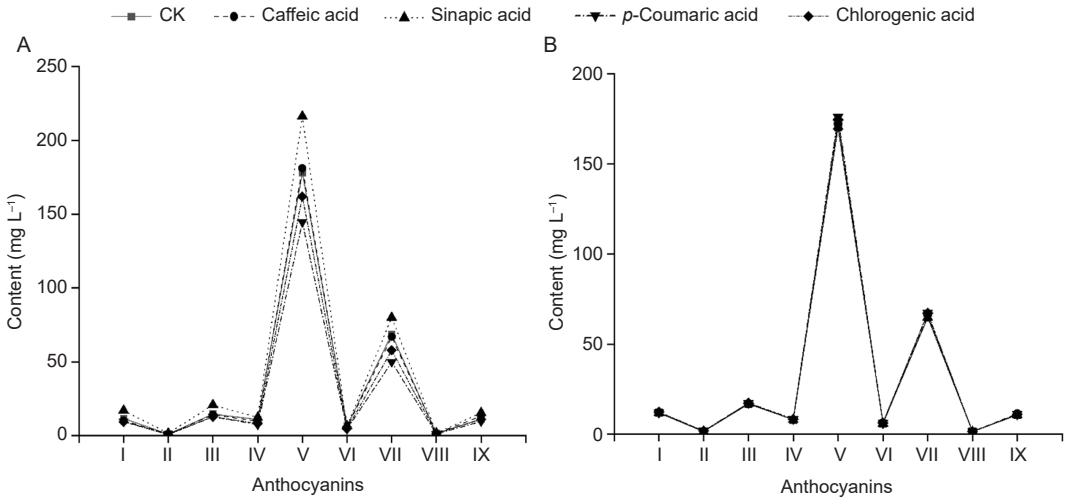


Fig. 2 Anthocyanin content of the real wine samples with the addition of hydroxycinnamic acids before fermentation (A) and after fermentation (B). I, delphinidin-3-*O*-glucoside; II, cyanidin-3-*O*-glucoside; III, petunidin-3-*O*-glucoside; IV, peonidin-3-*O*-glucoside; V, malvidin-3-*O*-glucoside; VI, peonidin-3-*O*-acetyl-glucoside; VII, malvidin-3-*O*-acetyl-glucoside; VIII, peonidin-3-*O*-coumaroyl-glucoside; IX, malvidin-3-*O*-coumaroyl-glucoside.

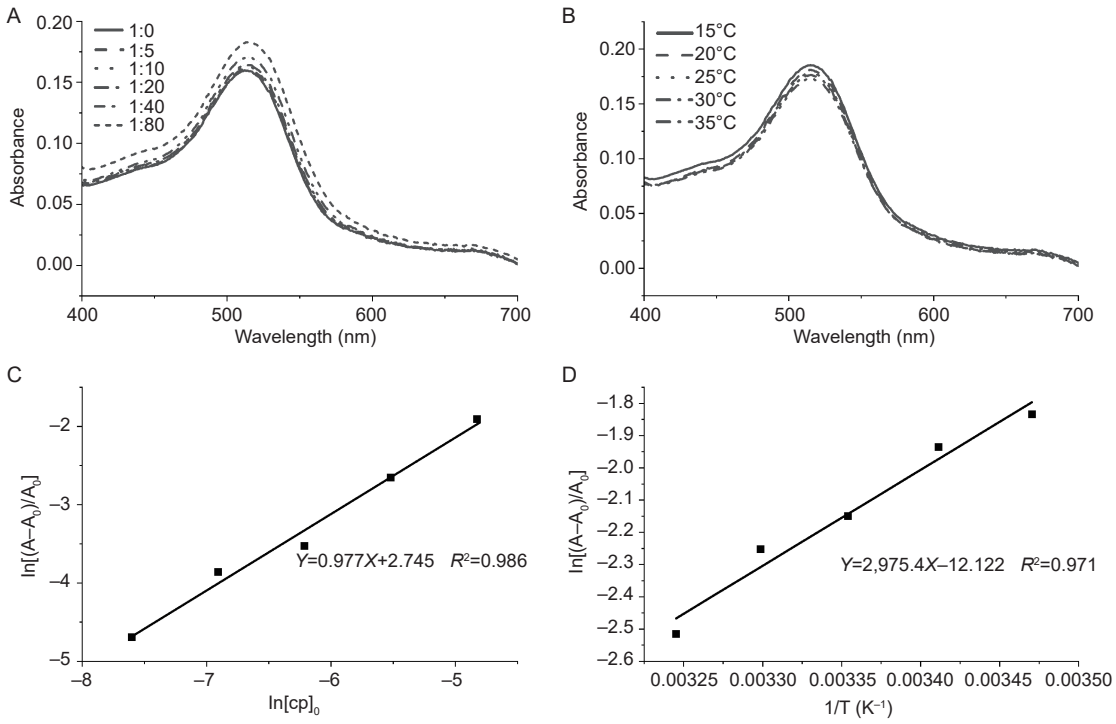


Fig. 3 Visible spectra and linear fitting function of sinapic acid/malvidin-3-*O*-glucoside. A, visible spectra at different molar ratios at 293 K. B, visible spectra at different temperatures. C, plots of ln $[(A–A_0)/A_0]$ *vs*. ln$[CP]_0$ for the copigmentation interaction. D, plots of ln$[(A–A_0)/A_0]$ *vs*. (1/T) for the copigmentation interaction.

a “translated-parallel” configuration (conformers 3 and 6) and an “aslant-parallel” arrangement (conformers 1, 2, 4, 5, and 7). The stacking distances between the planes of the conformers ranged from 3.43 Å to 4.47 Å, with dihedral angles spanning 4.00° to 6.80° in the translated-parallel mode and 10.06° to 18.70° in the aslant-parallel mode. Misalignment angles ranged from 11.27° to 43.35°, where smaller values corresponded to stronger π–π stacking. For conformer 6, these parameters were 3.43 Å, 4.00°, and 16.91°, respectively, reflecting its optimized stability.

HB plays a critical role in the stability of the copigmentation complexes, with 0 to 4 hydrogen bonds observed among the seven conformers. The most prominent interactions involved O-H···O bonds, with occasional contributions from C-H···O interactions. Hydrogen bond lengths ranged from 1.80 Å to 2.49 Å, and bond angles extended from 139.64° to 178.77°. Conformer 3, with its four HBs, exemplifies the importance of these interactions in maintaining structural stability. The 2′-COOH group of sinapic acid is essential in conformers 2, 4, and 6, while the 4-OH and 3,5-OCH_3 groups contribute significantly to conformers 3 and 5. Additionally, the 6′′-OH and 2′′-OH groups in the glucosyl moiety of anthocyanin are consistently critical for HB formation across all conformers. Parameters characterizing these HBs are annotated in Fig. 4 and Appendix D and summarized in Table 3.

Non-covalent interactions, including HB and dispersion forces, are illustrated in Fig. 4 and Appendix D. In conformer 6, a hydrogen bond (visualized as a blue isosurface) formed between the 2′-COOH group of sinapic acid and the 5′-OCH_3 group of malvidin-3-*O*-glucoside. The sign(λ_2)ρ value of this interaction was approximately –0.03, closely aligning with the –0.028 observed in the most stable structure of the caffeic acid and malvidin-3-*O*-glucoside complex (Wu *et al.* 2024a). Green isosurfaces indicate dispersion interactions, which contribute to the stabilization of conformer 6.

Binding energy analysis of copigmentation systems The thermal energy (Δ*E*), enthalpy (Δ*H*), Gibbs free energy (Δ*G*), and entropy (Δ*S*) for the seven lowest-energy conformers are summarized in Table 4, along with the experimentally derived Gibbs free energy values for comparison. Thermal energy ranged from –14.48 to –20.87 kcal mol^{-1}, indicating consistent electronic interactions between malvidin-3-*O*-glucoside and sinapic acid. These parameters are comparable to the previously reported values for the interaction of anthocyanin with caffeic acid (Wu *et al.* 2024a). Entropy effects tend to diminish intermolecular interactions, leading to increased order within the system. The Δ*G* ranged from –1.09 to –7.17 kcal mol^{-1}, indicating a thermodynamically favorable and spontaneous association between the two molecules.

The Boltzmann weight (*BW*) of each conformer, presented in Table 4, highlights conformers 5 and 6 as the predominant forms observed experimentally. Dispersion contributions within the sinapic acid and malvidin-3-*O*-glucoside complex ranged from –15.69 to –20.76 kcal mol^{-1}, as detailed in Table 4.

4. Discussion

4.1. Effect of hydroxycinnamic acid on the chromatic features of wine at different periods

The chromatic characteristics of the final wine samples

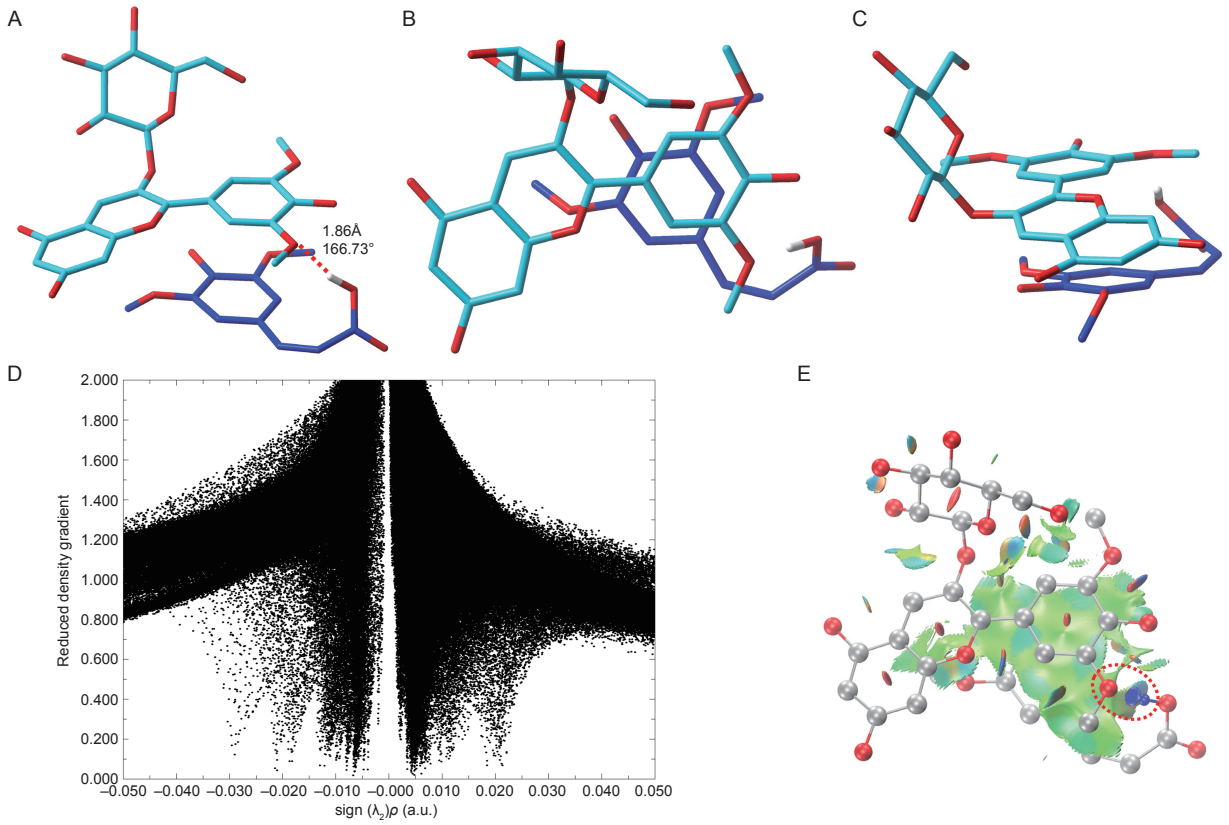


Fig. 4 Molecular structure and non-covalent interactions in conformer 6 of the sinapic acid/malvidin-3-*O*-glucoside complex. A–C, front, side, and top views showing hydrogen bonds (red dashed) and key parameters. D and E, visualization of non-covalent interactions with isosurface (s=0.5 a.u.).

Table 3 Hydrogen bonding (HB) and ring stacking (RS) parameters for the sinapic acid/malvidin-3-*O*-glucoside (distance in angstrom, angle in degree)

Conformer	HB (D-H…A)[1]				RS			
	Quantity	Type	*r*(H…A)[2]	∠(D-H…A)[3]	Type[4]	*r*(RS)[2]	∠(RS)[3]	∠(MS)[5]
1	0				C…S	3.55	15.24	11.27
2	2	O-H…O	1.85	172.91	AC…S	4.01	18.56	43.35
3	4	O-H…O C-H…O	1.80	140.89	A…S	3.67	6.80	19.46
4	2	O-H…O	1.84	178.77	AC…S	4.02	18.70	42.02
5	1	O-H…O	1.92	139.64	–	4.47	13.26	36.39
6	1	O-H…O	1.86	166.73	B…S	3.43	4.00	16.91
7	0				C…S	3.74	10.06	22.80

[1] Parameters are presented only for the strongest hydrogen bond, while the others are displayed in Fig. 3 and Appendix D. D and A represent the hydrogen donor and acceptor, respectively.
[2] Distance between H and A or between the two rings.
[3] Angle of a hydrogen bond or dihedral angle between two rings.
[4] B, C, AC, and S denote the B-ring, C-ring, AC-ring of malvidin-3-*O*-glucoside, and the S-ring of sinapic acid.
[5] The angle between the normal vectors of the planes of malvidin-3-*O*-glucoside and the line connecting the geometric centers of the two planes is referred to as the angle of misalignment, which reflects the degree of relative misalignment.

underwent a substantial change when phenolic acids were added prior to fermentation (Table 1). Specifically, increases in L^*, a^*, and C^*_{ab} of the hydroxycinnamic acid-treated samples indicated enhanced color intensity, which indicates that hydroxycinnamic acids contributed positively to the color of Cabernet Sauvignon dry red wine (Liu *et al.* 2024). This is consistent with previous findings highlighting the critical role of phenolics in stabilizing wine color (Rivero *et al.* 2017). Phenolic acid was added before fermentation, and as fermentation proceeded, the anthocyanins in the raw grapes were gradually leached. Compared with CK, the treatment group with higher initial concentrations of hydroxycinnamic acids had greater capacity to bind free anthocyanins, resulting in more stable and intensely colored complexes.

Similarly, post-fermentation addition of hydroxycinnamic acids had a positive effect on the chromatic features of samples. Compared with CK, the treated samples exhibited higher redness, lower yellowness, and better color

Table 4 Binding energetics (Δ*E*, Δ*H*, Δ*G*, Δ*S*), Boltzmann weights (*BW*) and dispersion energy ($\Delta E_{dispersion}$) for the sinapic acid/malvidin-3-*O*-glucoside complexes[1)]

Conformer	Δ*E*	Δ*H*	Δ*G*	Δ*S*	*BW*	$\Delta E_{dispersion}$
1	–14.48	–15.07	–1.09	–196.14	0.00	–20.76
2	–20.20	–20.79	–5.16	–219.30	2.51	–17.80
3	–18.32	–18.91	–5.51	–187.95	4.55	–15.96
4	–20.26	–20.85	–5.26	–218.81	2.96	–17.80
5	–19.75	–20.34	–6.22	–198.18	14.89	–19.12
6	–20.87	–21.46	–7.17	–200.64	74.03	–17.19
7	–17.31	–17.90	–4.65	–185.96	1.05	–17.28
Expt.[2)]			–1.63			

[1)] Energy (Δ*E*, Δ*H*, Δ*G*, $\Delta E_{dispersion}$) in kcal mol^{-1}; entropy (Δ*S*) in J K^{-1} mol^{-1}; *BW* is calculated based on the Δ*G*, in %.
[2)] Experimental value calculated from the thermodynamic data.

saturation (Table 2), which is associated with younger wines. These results provide further evidence that the addition of hydroxycinnamic acids can stabilize the color of Cabernet Sauvignon wines. The superior copigmentation performance of hydroxycinnamic acids may be related to the longer carbon chain of acrylic acid, which makes the molecule more flexible and more favorable for adopting a spatial conformation for the binding of copigments to anthocyanins (Malaj *et al.* 2013).

Compared to the data before fermentation, the spectral characteristics (Fig. 1) and monomeric anthocyanin content (Table 2) of treated samples after fermentation were less variable and did not differ significantly from CK. Maceration, fermentation, and aging conditions affect the anthocyanin composition of the wine, resulting in a change in the color of the wine (Gao *et al.* 1997). During wine fermentation, anthocyanins gradually change from a free state to macromolecules such as polymerized forms, which are less likely to combine with polyphenols. During aging, the content of free anthocyanins in wine gradually decreases, resulting in a decline in color (Xue *et al.* 2021). Therefore, the impact of polyphenols added after fermentation would be less significant. However, as aging progresses, copigmentation may gradually play a more important role in the color of wine samples. Some studies have shown that the non-covalent interaction between anthocyanins and polyphenols serves as the first step in the formation of covalent bonds, leading to the production of new anthocyanin derivatives that stabilize the color (Brouillard and Dangles 1994). This type of anthocyanins is believed to have a darker color, and its molar extinction coefficient has also been shown to be greater than that of monomeric anthocyanins (Håkansson *et al.* 2003).

4.2. Effect of hydroxycinnamic acid addition on the phenolic content of wine samples at different periods

The external color change of wine is primarily caused by alterations in pigmented substances (phenols) (Zhang *et al.* 2022). The addition of phenolic acids at different fermentation periods increased the total phenolic content of wine samples, which was higher than the addition of exogenous phenolic acids (Table 3), as well as the flavonol content of phenolic acid-treated samples at different fermentation periods. A similar phenomenon was found with the addition of other phenolic acids (Wu *et al.* 2024a, b). We hypothesized that the explanation for this phenomenon might be that the addition of phenolic acids facilitated the extraction of phenolic compounds from the wine solution.

In addition, the effect of exogenous phenolic acids on anthocyanin, an extremely important pigment, determines the color expression of the finished wine (Khoo *et al.* 2017). From Fig. 2 and Table 3, it is possible to note that the addition of phenolic acids before fermentation had a significant effect on the anthocyanin content, especially sinapic acid. The growth of the delphinidin-3-*O*-glucoside, petunidin-3-*O*-glucoside, malvidin-3-*O*-glucoside, and malvidin-3-*O*-acetylglucoside of the wine samples were particularly significant after the addition of sinapic acid. These monomeric anthocyanins were shown to correlate with *L**, *a** and *b** values, in agreement with the experimental results in previous studies (Han *et al.* 2008, 2009; Zezulová *et al.* 2021).

The data on the forms of anthocyanins in the wine samples indicated that the pre-fermentation addition of sinapic acid and caffeic acid significantly increased the proportions of copigmented anthocyanins compared with CK, and similar results were observed with the addition of other types of phenols (Aleixandre-Tudó *et al.* 2013; Rivero *et al.* 2017; Wu *et al.* 2024a, b). This observation supports the hypothesis that the exogenously added phenolic acids actively participate in copigmentation interactions, stabilizing the structure of anthocyanins and enhancing color quality.

The amount of exogenous phenolic acid added is another concern. Previous studies have also shown that the addition of polyphenols affected the activity of yeast (Mekoue Nguela *et al.* 2019). It was reported that the growth and metabolic disorders of yeast caused by polyphenolic compounds may be mainly related to their interaction with the plasma membrane of yeast cells. From the results of this study, it can be speculated that polyphenols may affect the activity of yeast, and because the reduced sugar content of grape was higher, a higher content of ethanol would be produced, resulting in the activity of yeast being affected by polyphenols and ethanol near the end of fermentation at the same time, then the reduced sugar of the treated wine samples was slightly higher than that of the control group. However, the fermentation time of each treatment group was basically the same as that of CK, and the indicators of the wine samples were not abnormal, indicating that the added amount of phenolic acid in this experiment was within a reasonable range.

4.3. Molecular mechanism of intermolecular copigmentation between malvidin-3-*O*-glucoside and sinapic acid

To further investigate the intrinsic mechanism of color enhancement by hydroxycinnamic acids in wine, a thermodynamic study was conducted using a model wine solution, and the results are presented in Fig. 3. The copigmentation interaction between sinapic acid and malvidin-3-*O*-glucoside was found to be spontaneous and exothermic, with Δ*G*, Δ*H*, and Δ*S* being negative. These results confirm that the interaction is enthalpy-driven, where Δ*H* is smaller than Δ*G*, Δ*S* is dominant, and the reaction

system becomes more organized, consistent with previous findings for copigmentation involving caffeic acid, syringic acid, and gallic acid (Li *et al.* 2019; Wu *et al.* 2024a, b). Additionally, the binding strength had a positive correlation with the content of copigments and a negative correlation with temperature. The results also indicated that the binding ratio of sinapic acid and malvidin-3-*O*-glucoside in the model wine was 1:1, which is consistent with previous findings that anthocyanins and copigments (flavonols, flavanols, phenolic aldehydes, and phenolic acids) are combined in a ratio close to 1:1 (Teixeira *et al.* 2013; Zhang *et al.* 2015b; Li *et al.* 2018; Wu *et al.* 2024a).

Insights from both real and model wines indicate that the copigmentation effect between hydroxycinnamic acid and anthocyanins is essential for enhancing the color expression of the solution. What is the molecular interplay mechanism of this interaction? Fig. 4 presents images of the interactions and the thermodynamics, which offer insights into the nature of the copigmentation effect.

The structure of the interaction between malvidin-3-*O*-glucoside and sinapic acid is clearly shown in Fig. 4 and Appendix D, along with specific parameters in Table 3. Malvidin-3-*O*-glucoside interacts with sinapic acid in a stacked form known as π–π stacking, as previously reported (Trouillas *et al.* 2016). In 7 conformers, the sinapic acid backbone interacts with 1 or 2 stacked anthocyanin rings. The most structurally stable conformer 6 was stacked only with the B ring at a distance of 3.43 Å, while the distances between the other conformers ranged from 3.55 to 4.47 Å. Based on the distances observed in the malvidin-3-*O*-glucoside/caffeic acid complexes, which are approximately 3.29 Å) (Wu *et al.* 2024a), in the malvidin-3-*O*-glucoside/gallic acid complex (~3.35 Å) (Wu *et al.* 2024b), in the malvidin-3-*O*-glucoside/syringic acid complex (~3.29 Å) (Li *et al.* 2019), it is possible to deduce that the optimum distance for the stacking interactions between anthocyanin and phenolic acids is 3.30–3.40 Å. In the most stable conformer 6, the dihedral angle between sinapic acid and anthocyanin is 4°, which is very close to the dihedral angle between caffeic acid and anthocyanin, 3.29° (Wu *et al.* 2024a), and similar angles are obtained for gallic acid and syringic acid, 2.45° and 1.57°, respectively (Li *et al.* 2019; Wu *et al.* 2024b). The difference, however, is that the stacking of the sinapic acid did not take place inside the anthocyanin (between the backbone and the glucoside). The optimal form of stacking for all phenolic acids is parallel, but the position of the copigments is not important. The backbones of the anthocyanins in all seven conformers have remained approximately parallel, which may be attributed to the stacking of the copigments with the anthocyanins limiting the rotation of the C-C bond between the B and C rings. Similar results were previously observed for caffeic acid, gallic acid, and syringic acid (Li *et al.* 2019; Wu *et al.* 2024a, b). However, the three rings of quercetin increase its flexibility when stacked with anthocyanins, and the C-C bond between the B and C rings rotates significantly when anthocyanins bind to it (Li *et al.* 2018). Therefore, it can be deduced that anthocyanins tend to present a planar skeleton (three benzene rings in a plane) when stacked with phenolic acid. In contrast, interactions with flavonoids often lead to the rotation of the C-C bonds connecting rings B and C in both anthocyanin and cofactor molecules, resulting in a non-planar configuration.

The structural characteristics of these complexes are closely related to their energetic properties. For the seven conformers of sinapic acid and malvidin-3-*O*-glucoside, the calculated Δ*G* of binding ranged from –1.09 to –7.17 kcal mol^{-1}, in good agreement with the experimental value of –1.63 kcal mol^{-1}, thereby confirming the spontaneity of the binding process, comparable to the interaction between malvidin-3-*O*-glucoside and caffeic acid (Wu *et al.* 2024a). Analysis of thermodynamic parameters (Table 4) revealed that the interaction is dominated by enthalpic contributions, with significant involvement of both HB and dispersion (Teixeira *et al.* 2013). Similar mechanisms have been reported for oenin/syringic acid complexes (Li *et al.* 2019) and oenin/quercetin complexes (Li *et al.* 2018).

HB interactions mainly stem from the carboxyl and phenolic hydroxyl groups of the copigments, while dispersion forces arise from stacking of the molecular backbones. The stability of the system is achieved through a balance of key geometric factors such as overlap, distance, parallelism, and planarity, optimizing both HB and dispersion contributions. Structural features and binding energies are thus mutually dependent.

Three critical outcomes arise from these interactions: (1) Color enhancement: Binding between sinapic acid and malvidin-3-*O*-glucoside induces a redshift in the absorption spectrum, enhancing the chromatic intensity of the system and, by extension, the wine. This is consistent with both experimental observations and theoretical predictions. (2) Molecular structural stability: The complex demonstrates greater resistance to degradation in wine solutions compared to individual molecules, as it is less vulnerable to external attacks (Boulton 2001; Trouillas *et al.* 2016). This stabilization results in either the preservation of the complex form or an increased proportion of derivatives such as polymeric anthocyanins (Wang *et al.* 2021). (3) Active binding sites: The 2′-COOH group in sinapic acid and the 6′′-OH group in malvidin-3-*O*-glucoside play pivotal roles in hydrogen bond formation. Phenolic hydroxyl and methoxyl groups in sinapic acid facilitate interactions with the sugar moiety of malvidin-3-*O*-glucoside. Similar hydrogen bond interactions have been reported for systems involving the 3′-OH in quercetin, the 2′-COOH in caffeic acid, the 1-COOH in syringic acid, and the 5-OH in gallic acid.

5. Conclusion

This study explored the effects of hydroxycinnamic acids on Cabernet Sauvignon wine's chromatic properties and phenolic composition, supported by thermodynamic and QM calculations. The important conclusions are as follows: (1) The four hydroxycinnamic acids selected in this study exerted positive effects on the color of wine samples, indicating that they possess significant auxiliary color potential. (2) Pre-fermentation addition is superior to post-fermentation treatment, though HCA amounts must be carefully controlled to avoid negatively affecting yeast activity. (3) Sinapic acid

proved most effective for anthocyanin stabilization, and the copigmentation was confirmed to be enthalpy-driven and spontaneous. (4) Theoretical calculations showed that the interactions between sinapic acid and anthocyanin were primarily driven by HB and dispersion. The backbones of the pigments and copigments were the main factors influencing dispersion, while the carboxyl groups in sinapic acid facilitate HB. In conclusion, this research refines the understanding of the copigmentation effect, offering valuable theoretical support for dry red wine color protection technology.

Acknowledgements

This work was supported by the Key R&D Program of Shaanxi Province, China (2024NC-YBXM-146), the Xi'an Agricultural Technology Research and Development Project, China (24NYGG0048), the Key R&D Program of Xianyang, China (L2024-ZDYF-ZDYF-NY-0028) and the National Foreign Expert Project of China (G2023172002L).

Declaration of competing interest

The authors declare that they have no conflict of interest.

Declaration of generative AI and AI-assisted technologies in the writing process

The authors declare that they did not use AI in the preparation and writing of this manuscript.

Appendices associated with this paper are available at https://doi.org/10.1016/j.jia.2025.10.013

References

Alcalde-Eon C, Escribano-Bailón M T, Santos-Buelga C, Rivas-Gonzalo J C. 2006. Changes in the detailed pigment composition of red wine during maturity and ageing: A comprehensive study. *Analytica Chimica Acta*, **563**, 238–254.

Aleixandre-Tudó J L, Álvarez I, Lizama V, García M J, Aleixandre J L, Du Toit W J. 2013. Impact of caffeic acid addition on phenolic composition of tempranillo wines from different winemaking techniques. *Journal of Agricultural and Food Chemistry*, **61**, 11900–11912.

Arnous A, Makris D P, Kefalas P. 2002. Correlation of pigment and flavanol content with antioxidant properties in selected aged regional wines from greece. *Journal of Food Composition and Analysis*, **15**, 655–665.

Bimpilas A, Panagopoulou M, Tsimogiannis D, Oreopoulou V. 2016. Anthocyanin copigmentation and color of wine: The effect of naturally obtained hydroxycinnamic acids as cofactors. *Food Chemistry*, **197**, 39–46.

Boulton R. 2001. The Copigmentation of Anthocyanins and its role in the color of red wine: A critical review. *American Journal of Enology and Viticulture*, **52**, 67–87.

Brouillard R, Dangles O. 1994. Anthocyanin molecular interactions: The first step in the formation of new pigments during wine aging? *Food Chemistry*, **51**, 365–371.

Brouillard R, Mazza G, Saad Z, Albrecht-Gary A M, Cheminat A. 1989. The co-pigmentation reaction of anthocyanins: A microprobe for the structural study of aqueous solutions. *Journal of the American Chemical Society*, **111**, 2604–2610.

Cliff M A, King M C, Schlosser J. 2007. Anthocyanin, phenolic composition, colour measurement and sensory analysis of BC commercial red wines. *Food Research International*, **40**, 92–100.

Escribano-Bailon M T, Santos-Buelga C. 2012. Anthocyanin copigmentation- evaluation, mechanisms and implications for the colour of red wines. *Current Organic Chemistry*, **16**, 715–723.

Fan S, Liu C, Li Y, Zhang Y. 2023b. Visual representation of red wine color: methodology, comparison and applications. *Foods*, **12**, 924.

Fan S, Zhang Y, Li Y, 2023a. A New Approach for Quantitative Classification of Red Wine Color from the Perspective of Micro and Macro Levels. *Fermentation*, **9**, 519.

Fanzone M, González-Manzano S, Pérez-Alonso J, Escribano-Bailón M T, Jofré V, Assof M, Santos-Buelga C. 2015. Evaluation of dihydroquercetin-3-*O*-glucoside from Malbec grapes as copigment of malvidin-3-*O*-glucoside. *Food Chemistry*, **175**, 166–173.

Fontana A R, Antoniolli A, Bottini R. 2013. Grape pomace as a sustainable source of bioactive compounds: Extraction, characterization, and biotechnological applications of phenolics. *Journal of Agricultural and Food Chemistry*, **61**, 8987–9003.

Frisch M J, Trucks G W, Schlegel H B, Scuseria G E, Robb M A, Cheeseman J R, Scalmani G, Barone V, Mennucci B, Petersson G A, Nakatsuji H, Caricato M, Li X, Hratchian H P, Izmaylov A F, Bloino J, Zheng G, Sonnenberg J L, Hada M, Ehara M, *et al.* 2009. Gaussian 09W, revision A. 02. Gaussian, Inc., Wallingford, CT.

Gao L, Girard B, Mazza G, Reynolds A G. 1997. Changes in anthocyanins and color characteristics of pinot noir wines during different vinification processes. *Journal of Agricultural and Food Chemistry*, **45**, 2003–2008.

Gonnet J F. 1999. Colour effects of co-pigmentation of anthocyanins revisited–2.A colorimetric look at the solutions of cyanin co-pigmented byrutin using the CIELAB scale. *Food Chemistry*, **66**, 387–394.

González-Manzano S, Dueñas M, Rivas-Gonzalo J C, Escribano-Bailón M T, Santos-Buelga C. 2009. Studies on the copigmentation between anthocyanins and flavan-3-ols and their influence in the colour expression of red wine. *Food Chemistry*, **114**, 649–656.

Grimme S, Antony J, Ehrlich S, Krieg H. 2010. A consistent and accurate ab initio parametrization of density functional dispersion correction (DFT-D) for the 94 elements H-Pu. *The Journal of Chemical Physics*, **132**, 154104.

Han F L, Jiang S M, He J J, Pan Q H, Duan C Q, Zhang M X. 2009. Anthocyanins in "Cabernet Gernischet" (*Vitis vinifera* L. cv.) aged red wine and their color in aqueous solution analyzed by partial least square regression. *Food Science and Biotechnology*, **18**, 724–731.

Han F L, Zhang W N, Pan Q H, Zheng C R, Chen H Y, Duan C Q. 2008. Principal component regression analysis of the relation between CIELAB color and monomeric anthocyanins in young Cabernet Sauvignon wines. *Molecules*, **13**, 2859–2870.

Håkansson A E, Pardon K, Hayasaka Y, de Sa M, Herderich M. 2003. Structures and colour properties of new red wine pigments. *Tetrahedron Letters*, **44**, 4887–4891.

Humphrey W, Dalke A, Schulten K. 1996. VMD: Visual molecular dynamics. *Journal of Molecular Graphics*, **14**, 33–38.

Ignat I, Volf I, Popa V I. 2011. A critical review of methods for characterisation of polyphenolic compounds in fruits and vegetables. *Food Chemistry*, **126**, 1821–1835.

Kent K, Charlton K E, Netzel M, Fanning K. 2017. Food-based anthocyanin intake and cognitive outcomes in human intervention trials: A systematic review. *Journal of Human Nutrition and Dietetics*: *The Official Journal of the British Dietetic Association*, **30**, 260–274.

Khoo H E, Azlan A, Tang S T, Lim S M. 2017. Anthocyanidins and anthocyanins: Colored pigments as food, pharmaceutical ingredients, and the potential health benefits. *Food & Nutrition Research*, **61**, 1361779.

Lambert S G, Asenstorfer R E, Williamson N M, Iland P G, Jones G P. 2011. Copigmentation between malvidin-3-glucoside and some wine constituents and its importance to colour expression in red wine. *Food Chemistry*, **125**, 106–115.

Li Y, Prejanò M, Toscano M, Russo N. 2018. Oenin and quercetin copigmentation: highlights from density functional theory. *Frontiers in Chemistry*, **6**, 245.

Li Y, Prejanò M, Toscano M, Russo N. 2019. Oenin/syringic acid copigmentation: insights from a theoretical study. *Frontiers in Chemistry*, **7**, 579.

Lingua M S, Fabani M P, Wunderlin D A, Baroni M V. 2016. From grape to wine: Changes in phenolic composition and its influence on antioxidant activity. *Food Chemistry*, **208**, 228–238.

Liu C, Wei X, Zhang Z, Miao Q, Prejanò M, Marino T, Tao Y, Li Y. 2025c. Color protection, aroma enhancement and sensory improvement of red wines: Comparison of pre-fermentation additions of cyclodextrins and polysaccharides. *Food Chemistry*, **477**, 143432.

Liu C, Wu L, Fan S, Tao Y, Li Y. 2024. The protective effect of cyclodextrin on the color quality and stability of Cabernet Sauvignon red wine. *Journal of Integrative Agriculture*, **23**, 310–323.

Liu C, Wu L, Zhang Z, Li Z, Prejanò M, Marino T, Tao Y, Li Y. 2025a. Copigmentation effect and mechanism of α-cyclodextrin on wine color quality and stability: Combining dynamics, thermodynamics, structural characterization and quantum mechanics. *Food Hydrocolloids*, **163**, 111068.

Liu C, Zheng F, Li H, Prejanò M, Jin G, Tao Y, Li Y. 2025b. Thermodynamics and quantum mechanical insights into benzoic acid-acetate ester interactions for aroma modulation and controlled release in wine. *Food Chemistry*, **483**, 144286.

Liu S X, Yang H Y, Li S Y, Zhang J Y, Li T, Zhu B Q, Zhang B L. 2015. Polyphenolic compositions and chromatic characteristics of bog bilberry syrup wines. *Molecules*, **20**, 19865–19877.

Lu T, Chen F. 2012. Multiwfn: A multifunctional wavefunction analyzer. *Journal of Computational Chemistry*, **33**, 580–592.

Malaj N, De Simone B C, Quartarolo A D, Russo N. 2013. Spectrophotometric study of the copigmentation of malvidin 3-O-glucoside with p-coumaric, vanillic and syringic acids. *Food Chemistry*, **141**, 3614–3620.

Mazza G, Fukumoto L, Delaquis P, Girard B, Ewert B. 1999. Anthocyanins, phenolics, and color of Cabernet Franc, Merlot, and Pinot Noir wines from British Columbia. *Journal of Agricultural and Food Chemistry*, **47**, 4009–4017.

Mekoue Nguela J, Vernhet A, Julien-Ortiz A, Sieczkowski N, Mouret J R. 2019. Effect of grape must polyphenols on yeast metabolism during alcoholic fermentation. *Food Research International*, **121**, 161–175.

Peri P, Kamiloglu S, Çapanoğlu E, Ozcelik B. 2015. Investigating the effect of aging on the phenolic content, antioxidant activity and anthocyanins in turkish wine. *Journal of Food Processing and Preservation*, **39**, 1845–1853.

Rivero F J, Gordillo B, Jara-Palacios M J, González-Miret K L, Heredia F J. 2017. Effect of addition of overripe seeds from white grape by-products during red wine fermentation on wine colour and phenolic composition. *LWT*, **84**, 544–550.

Simon S, Duran M, Dannenberg J J. 1996. How does basis set superposition error change the potential surfaces for hydrogen-bonded dimers? *The Journal of Chemical Physics*, **105**, 11024–11031.

Sun L, Warren F J, Gidley M J, Guo Y, Miao M. 2019. Mechanism of binding interactions between young apple polyphenols and porcine pancreatic α-amylase. *Food Chemistry*, **283**, 468–474.

Teixeira N, Cruz L, Brás N F, Mateus N, Ramos M J, de Freitas V. 2013. Structural features of copigmentation of oenin with different polyphenol copigments. *Journal of Agricultural and Food Chemistry*, **61**, 6942–6948.

Trouillas P, Sancho-García J C, De Freitas V, Gierschner J, Otyepka M, Dangles O. 2016. Stabilizing and modulating color by copigmentation: Insights from theory and experiment. *Chemical Reviews*, **116**, 4937–4982.

Wang X, Li Y, Song H, Tao Y, Russo N. 2021. Phenolic matrix effect on aroma formation of terpenes during simulated wine fermentation-part I: Phenolic acids. *Food Chemistry*, **341**, 128288.

Wu L, Prejanò M, Russo N, Tao Y, Marino T, Li Y, 2026. Ethanol-Dependent Solvent effects on copigmentation between oenin and quercetin: Insights from spectroscopy, thermodynamics and molecular simulations. *Journal of Molecular Structure*, **1353**, 144579.

Wu L, Zhang Y, Fan S, Prejanò M, Marino T, Russo N, Tao Y, Li Y. 2024a. Intermolecular interactions between malvidin-3-*O*-glucoside and caffeic acid: Structural and thermodynamic characterization and its effect on real wine color quality. *Food Chemistry*, **453**, 139617.

Wu L, Zhang Y, Prejanò M, Marino T, Russo N, Tao Y, Li Y. 2024b. Gallic acid improves color quality and stability of red wine via physico-chemical interaction and chemical transformation as revealed by thermodynamics, real wine dynamics and benchmark quantum mechanical calculations. *Food Research International*, **188**, 114510.

Wu L, Zheng F, Li H, Prejanò M, Marino T, Russo N, Tao Y, Li Y. 2025. Effect of hydroxycinnamic acids on ester-improving and aroma-enhancing of Cabernet Sauvignon red wine and its mechanism. *Food Research International*, **217**, 116763.

Xue Z D, Zhang Q A, Wang T T. 2021. Co-pigmentation of caffeic acid and catechin on wine color and the effect of ultrasound in model wine solutions. *Journal of AOAC International*, **104**, 1703–1709.

Zezulová E, Göttingerová M, Kiss T, Ondrášek I, Venuta R, Wolf J, Necas T. 2021. CIELAB analysis and quantitative correlation of total anthocyanin content in European and Asian plums. *European Journal of Horticultural Science*, **86**, 453–460.

Zhang B, He F, Zhou P P, Liu Y, Duan C Q. 2015a. Copigmentation between malvidin-3-*O*-glucoside and hydroxycinnamic acids in red wine model solutions: Investigations with experimental and theoretical methods. *Food Research International*, **78**, 313–320.

Zhang B, Liu R, He F, Zhou P P, Duan C Q. 2015b. Copigmentation of malvidin-3-*O*-glucoside with five hydroxybenzoic acids in red wine model solutions: Experimental and theoretical investigations. *Food Chemistry*, **170**, 226–233.

Zhang X K, Jeffery D W, Li D M, Lan Y, Zhao X, Duan C Q. 2022. Red wine coloration: A review of pigmented molecules, reactions, and applications. *Comprehensive Reviews in Food Science and Food Safety*, **21**, 3834–3866.

Executive Editor-in-Chief Qiang Wang
Managing Editor Lingyun Weng